JP4.8 LONGWAVE COOLING RATES IN INHOMOGENEOUS STRATOCUMULUS CLOUDS: 3D RADIATION TRANSFER VERSUS INDEPENDENT PIXEL APPROXIMATION CALCULATIONS

Mikhail Ovtchinnikov[1], David B. Mechem[2], Thomas P. Ackerman[1], Robert F. Cahalan[3], Anthony B. Davis[4], Robert G. Ellingson[5], K. Franklin Evans[6], Yefim L. Kogan[2], and Ezra E. Takara[5]

[1]Pacific Northwest National Laboratory, Richland, Washington
[2]Cooperative Institute for Mesoscale Meteorological Studies, University of Oklahoma, Norman, Oklahoma
[3]NASA/Goddard Space Flight Center, Greenbelt, Maryland
[4]Los Alamos National Laboratory, Los Alamos, New Mexico
[5]Florida State University, Tallahassee, Florida
[6]University of Colorado, Boulder, Colorado

1. INTRODUCTION *

We are concerned with 3-D effects of longwave (thermal or IR) radiative transfer through inhomogeneous clouds. In cloud models, IR RT is typically calculated under the Independent Pixel Approximation (IPA), which may not properly account for horizontal variability.

We seek to advance previous studies whose limitations included:

- use of highly simplified cloud shapes;
- assuming homogeneous internal structure of clouds;
- estimating total LW heating rates from a single wavelength or a single band calculation.

In this study, we seek to relax these limitations by performing broadband RT calculation using the SHDOM with correlated k-distribution on a realistic cloud fields generated by a large-eddy simulation model. We will analyze instantaneous 3D broadband longwave cooling rates in a simulated stratocumulus cloud and, in particular, the differential heating rate (***dhr***)

$$\boldsymbol{dhr} = (dT/dt)_{3D} - (dT/dt)_{IPA} .$$

The cloud type is chosen because IR cooling is the primary forcing for sustaining stratocumulus clouds. This "frozen cloud" study is a first step toward our ultimate goal of studying interaction between micro- and macro-physical cloud properties and 3-D radiative effects that implies accounting for multiple feedbacks in a dynamical framework.

2. MODEL SETUP

The radiative transfer (RT) model used in this study is the Spherical Harmonics Discrete Ordinate Method (SHDOM) by Evans (1998). SHDOM is a robust and extensively tested code although most validation efforts have been focused on shortwave monochromatic calculations.

In calculation presented here, the longwave spectrum (wavelength longer than 4 microns) is divided into twelve broad bands for which the radiative transfer (RT) is calculated with a correlated k-distribution (Fu and Liou 1992). The bounding wavelengths and wave numbers for each broad band are shown in Table 1. The SHDOM RT model accounts for thermal emission, absorption, and scattering, and its output includes hemispheric fluxes and the net flux convergence converted to heating rate.

The cloud field (i.e., the 3D distribution of the liquid water content) was generated using a large eddy simulation model. The spatial resolution of the LES model is 40 m in horizontal and 25 m in vertical. The computational domain contains 50 x 50 x 50 grid points to cover the 2 x 2 x 1.25 km^3 physical domain. The cloud top is at about 700-m level.

In RT calculation, the lower 32 levels coincide with the cloud model levels (0 to 775 m altitude) while the rest of the atmosphere is represented by seven additional levels taken from the standard atmosphere profile. All additional levels are horizontally uniform. Both LES model and SHDOM assume periodicity in ***x*** and ***y*** directions.

3. AVERAGE PROFILES

Because we expect the 3D effects to be relatively small (on the order of a few percent), a high accuracy is required for cooling rate calculations. The difference between IPA and 3D results includes real (physical) and artificial (numerical) components. The latter can be evaluated in a horizontally homogeneous case, where the two solutions should be physically identical.

3.1 *Horizontally Homogeneous Cloud*

Figure 1 shows the profiles of the upward and downward hemispheric fluxes and the cooling rate from 3D calculations as well the IPA deviations from these profiles. The calculation are performed using 128 discrete ordinates (8 zenith and 16 azimuth angles) and the following set of SHDOM accuracy parameters:

* *Corresponding author address*: Mikhail Ovtchinnikov, Pacific Northwest National Laboratory, P.O. Box 999, Mail Stop K9-24, Richland, WA 99352; e-mail: mikhail@pnl.gov

SPLITACC=5, SHACC=1, SOLACC=1.0e^{-4}. The differences in fluxes between 3D and IPA runs are virtually nonexistent below 600-m level. The 3D calculations predict larger (by ~1.5 W m^{-2}) downward flux at the top of PBL compared to the IPA. The reason for the discrepancy is not known but may be related to coarse vertical resolution in the free atmosphere (above the finely resolved boundary layer). This extra downward flux is absorbed near the cloud top, thus reducing the maximum cooling rate by ~0.1 K hr^{-1} in the 3D run compared the IPA. This is illustrated by a sharp peak in the difference between the two runs at 700 m level (Fig. 1). Absolute value of the discrepancy is much smaller in the rest of the domain. Although the relative errors in the heating rate can be up to 5%, in regions where the heating rates are nonnegligible (at the surface and near cloud base and cloud top) the relative errors are on the order of one percent. Other familiar features of the heating rate profile include a subtle warming just above the cloud base by surface emitted radiation and a slight cooling above the cloud. The latter is caused in part by use of the cooler standard atmosphere profile above the relatively warm boundary layer.

Sensitivity studies show that doubling the angular resolution to 16 zenith and 32 azimuth angles with simultaneous reduction of the accuracy parameters (SPLITACC=2, SHACC=0.4, SOLACC=0.5e^{-4}) does not notably improve the accuracy of the calculation, and neither does doubling the number of layers in the free atmosphere. The numerical bias in the heating rate shown in Fig 1 appears to be systematic, at least for the temperature, moisture, and liquid water profiles typical of a stratocumulus-topped boundary layer, with 3D RT calculations resulting in smaller cooling than IP approximation.

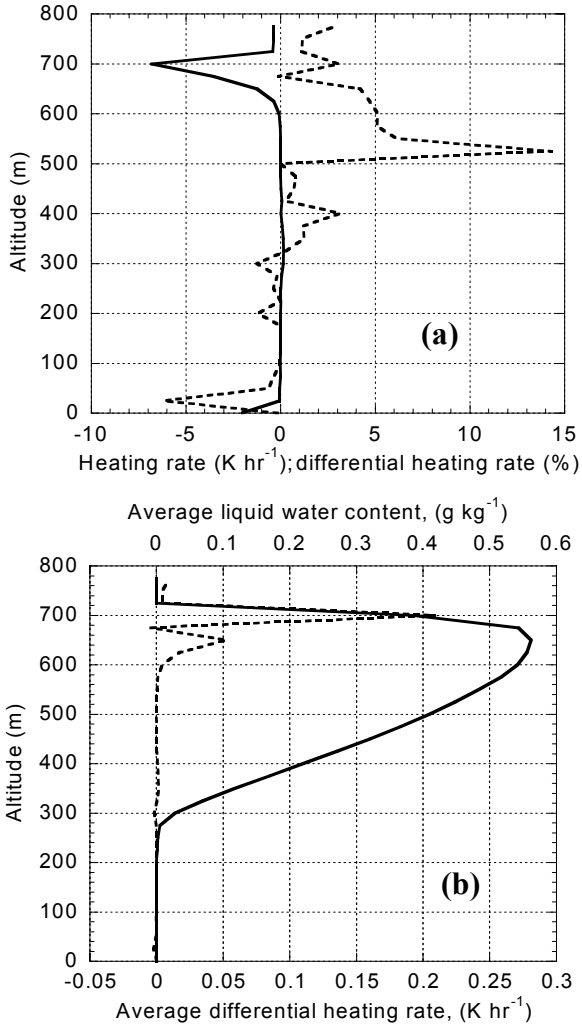

Fig 1. Average profiles of the heating rate (a, solid), relative (a, dashed) and absolute (b, dashed) differential heating rates, and liquid water content (b, solid) for the horizontally homogeneous cloud.

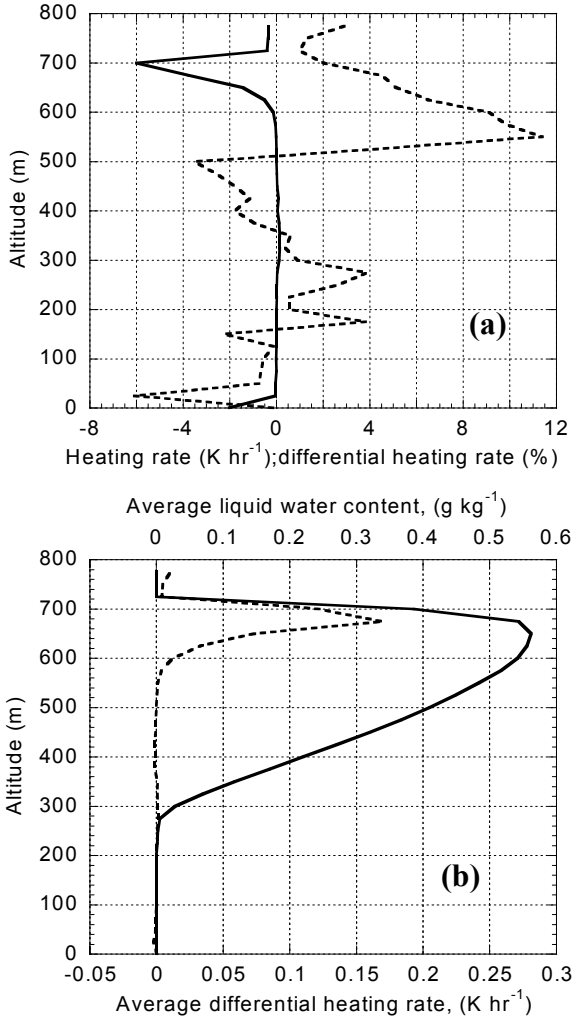

Fig 2. Same as Figure 2 but for inhomogeneous case.

3.2 *Horizontally Inhomogeneous Cloud*

We now consider the case when the cloud water field is variable in horizontal as well as in vertical. First, we look at horizontally averaged vertical profiles (Fig. 2). As expected, averaging over many columns with different cloud water content profiles results in a thicker layer of significant cooling and smaller averaged maximum cooling rate than in the previous case.

The vertical profiles of the upward and downward hemispheric fluxes are very similar to those in the homogeneous case and are not shown.

The maximum average difference between 3D and IP heating rates is very similar to that in the horizontally homogeneous case and may contain a physical bias from 3D effects in addition to the previously discussed numerical bias. It appears that the 3D treatment of LW RT results in a slightly weaker averaged cooling compared to the IPA. This would support the speculation by Guan et al. (1995) that radiative effects of up and down cloud top perturbations do not cancel each other out. The effect, however, is comparable to the overall accuracy of the presented results and thus cannot be quantified.

The local LW heating rates are much more sensitive to the approximations used in solving the RT.

4. PROBABILITY DISTRIBUTION OF THE DIFFERENTIAL HEATING RATE

Although the maxima of horizontally average ***dhr*** for homogeneous and inhomogeneous cases are similar and small (<0.2 K hr^{-1}, figs.1b, 2b), local ***dhr*** reach much higher values.

Fig. 3 illustrates the differences in ***dhr*** frequency distributions over all cloudy points. Both pdf are highly peaked near zero indicating that for a majority of the grid points there is no significant bias in heating rates in either case. In the horizontally homogeneous case, the pdf has a notably discrete structure. The two sharp peaks around 0.05 and 0.2 K hr^{-1} are due to confinement of the "homogeneous" bias to the two layers near the cloud top (fig. 1b). In the inhomogeneous case, the pdf still peaks at zero but has large wings on either side. With added horizontal variability the pdf becomes smoother, except for larger ***dhr***, where the statistics is less stable (***dhr*** was sampled at 0.01 K hr^{-1} intervals).

Cumulative probability distributions (fig. 4) further illustrate the frequency of occurrence of large ***dhr*** values. Note that there are ~40,000 cloudy grid points in the domain with each carrying a weight of ~0.0025%. For the homogeneous case, the bias is negligible for 88% of the points and is positive (0.2 K hr^{-1}) for the cloud-top layer (1 out of 17 cloud layers accounts for 6% of the points). For the inhomogeneous case, negative bias is found in 10% of the points. It is stronger than -0.4 K hr^{-1} in 1% and exceeds -1 K hr^{-1} only in 0.1 % of the total number of cloudy points. A positive bias is larger than the homogeneous maximum of 0.2 K hr^{-1} in 5% and exceeds 1 K hr^{-1} in 1 % of the points.

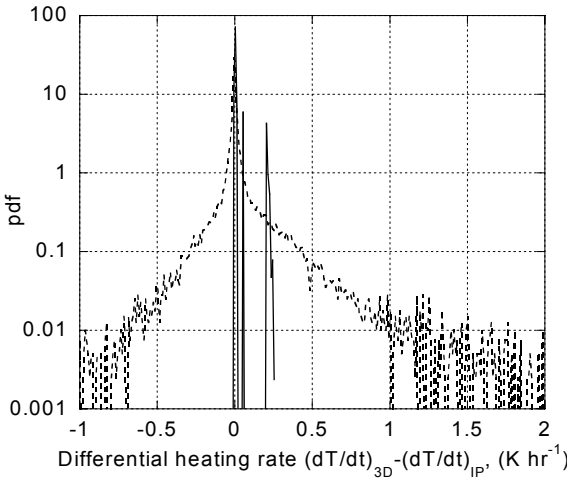

Fig 3. Normalized probability density function of the differential heating rate for horizontally homogeneous (solid) and inhomogeneous (dashed) cloud fields.

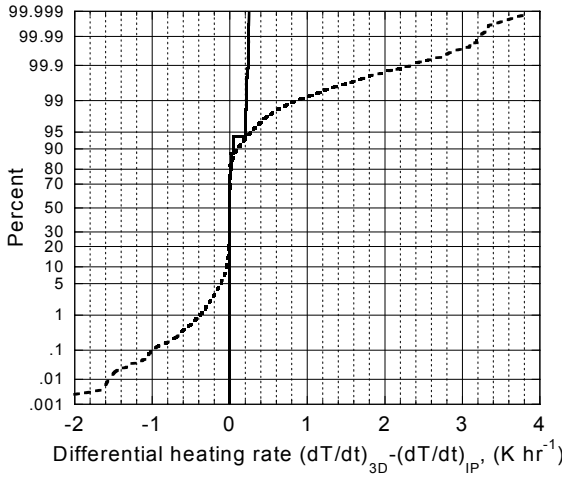

Fig 4. Cumulative probability distribution of the differential heating rate for horizontally homogeneous (solid) and inhomogeneous (dashed) cloud fields.

4. SPATIAL DISTRIBUTION OF THE DIFFERENTIAL HEATING RATE

The ***drh*** at *Z*=675m (fig.5a) is highly correlated with the liquid water content at *Z*=700m (fig.5b). The latter can also be viewed as a proxy for cloud top height (the higher LWC at this level the higher the cloud top).

Every depression in cloud top has a corresponding local maximum of the ***drh***, meaning that the cloud top there experiences less cooling in 3DRT simulation. In contrast, the local minima of the ***drh***, occur not on the surface but in the interior of the convex cloud top perturbations (humps) (fig. 6).

Areas of positive and negative ***drh*** are often located next to each other. The cumulative dynamic effect therefore will strongly depend on the efficiency of mixing between adjacent grid points.

There is no measurable difference in heating rates between 3D and IPA RT calculations in the interior of the cloud (below 625 m).

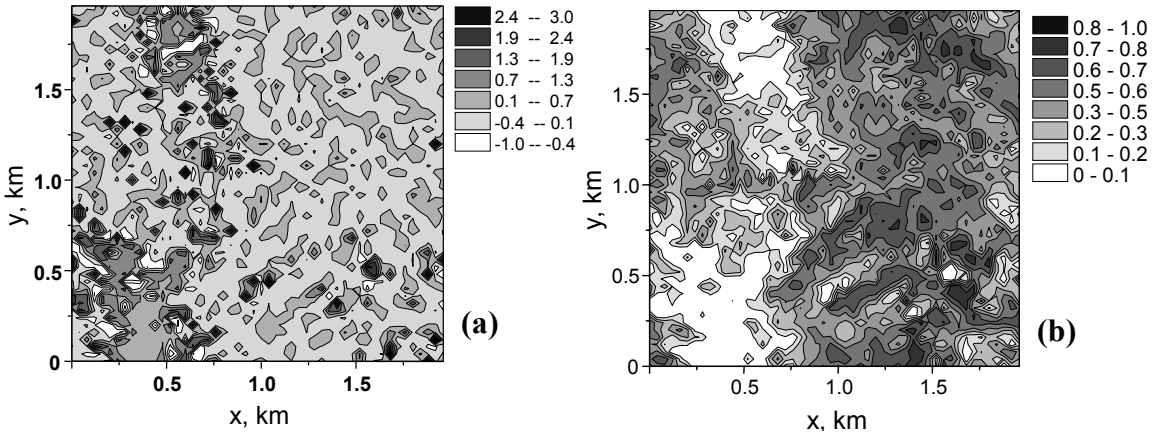

Fig. 5. Horizontal cross sections of the differential heating rate at Z = 675m (a) and liquid water content at Z= 700m (b).

5. DISCUSSION

The 3D effects in the instantaneous broadband longwave radiative heating rates presented here may affect cloud evolution but this can only be studied within the dynamical model framework that accounts for cloud-radiation feedback. We can speculate that weaker cooling of the surface of cloud top depressions and stronger cooling of the interior of the cloud top humps could have a stabilizing effect on the cloud top in a simulation that employ 3D RT. This in turn may result in suppressed entrainment and potentially more persistent cloud layer.

There is a known positive feedback between cloud top perturbations and longwave radiative cooling (Guan et al. 1995). Under depressions cloud cools more rapidly and under cloud top bumps cloud cools less rapidly than the unperturbed cloud region at the same level, thus promoting growth of these disturbances (Fig. 6). The 3D radiative effects weaken this feedback.

The spatial resolution of the presented cloud simulations (Δx = Δy = 40 m and Δz = 25 m) is typical for LES models and considered to be quite adequate to resolve main features of the cloudy PBL. Recent studies indicate, however, that this resolution may not be enough to reproduce the inversion strength and capture variations in inversion thickness and cloud top height (Stevens and Bretherton 1999). Refined resolution is therefore highly desired in future simulations.

6. ACKNOWLEDGEMENTS

This research was supported by the Environmental Sciences Division of the U.S. Department of Energy as part of the Atmospheric Radiation Measurement (ARM) Program.

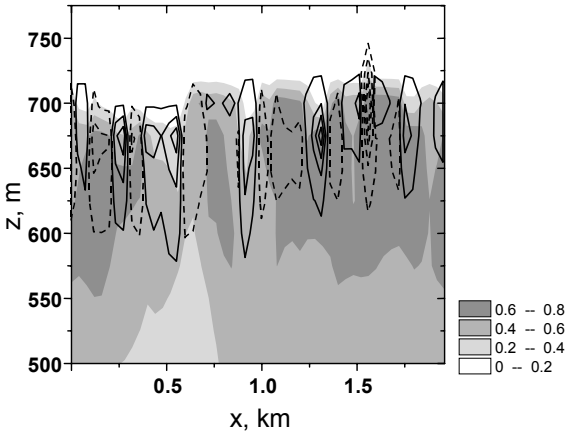

Fig 6. Vertical cross sections at y = 0.4 km of liquid water content (shaded) and positive (solid contours) and negative (dashed contours) differential heating rate at 0.5 K hr^{-1} interval. Only upper half of the cloud layer is shown to enhance details.

7. REFERENCES

Evans, K. F., 1998: The spherical harmonics discrete ordinate method for three-dimensional atmospheric radiation transfer. *J. Atmos. Sci.,* **55**, 429-446.

Fu, Q., and K. N. Liou, 1992: On the correlated k-distribution method for radiative transfer in nonhomogeneous atmospheres. *J. Atmos. Sci.,* **49**, 2139-2156.

Guan, H., R. Davies, and M. K. Yau, 1995: Longwave cooling rates in axially symmetric clouds. *J. Geophys. Res.,* **100**, 3213-3220.

Stevens, D. E., and C. S. Bretherton, 1999: Effects of resolution on the simulation of stratocumulus entrainment. *Quart. J. Roy. Meteor. Soc.,* **125**, 425-439.